ПРИБОРЫ И ТЕХНИКА ЭКСПЕРИМЕНТА, 2013, № 1, с. 115–123

ЛАБОРАТОРНАЯ ТЕХНИКА

FREQUENCY ADAPTIVE DRIVER FOR ULTRASONIC VIBRATORS WITH MOTIONAL CURRENT FEEDBACK

© 2013 г. C.-C. Wen[a, b], F.-L. Wen[c], C.-H. Lin[b]

[a] Department of Electronics Engineering, Ta Hwa of Institute Technology, Hsinchu County 307, Taiwan

[b] Department of Electrical Engineering, Tatung University, Taipei City 104, Taiwan

[c] Department of Mechanical & Computer-Aided Engineering/Graduate Institute of Automation & Mechatronics, St. John's University/Taipei Campus, Tamsui District, New Taipei City 25135, Taiwan

E-mail: ericwen@mail.sju.edu.tw

Received February 1, 2012

A driving circuit of frequency adapting for an ultrasonic vibrator with motional current feedback has been presented in this paper. Via a voltage-controlled oscillator (VCO) and a digital/analog converter (DAC), the driving signal would be magnified by a linear power amplifier to actuate the vibrator. Since the vibrating velocities or displacements at the surface end of a vibrator could be predicted through the measurement of motional current, the motional current passing through the vibrator was detected by a current transformer (CT) type sensor as feedback to monitor the optimal level of output power. The calculation for phase difference and the tuning strategy for driving frequency were implemented by a microcontroller integrated with an A/D converter and a voltage comparator as well as the signal attenuation and level tuning circuit. The experiment demonstrates that the temperature effect corresponding to frequencies is at 9.75 Hz/°C shifting and the external loading reflected to frequencies is about 8.3 Hz/gm offset. The proposed circuit has the great performance in rejecting the disturbances from external loading and thermal effect.

DOI: 10.7868/S0032816213010138

1. INTRODUCTION

An ultrasonic vibrator comprises two piezoelectric rings abutting against each other with two copper electrodes. This vibrator could be assembled with metal horns to gain larger vibrating amplitudes and to produce the specific deflection in longitudinal or transverse direction, called as a bolt-clamped Langevin vibrator (BLT). Hence, the BLT vibrator has high mechanical quality factor (Q_m: detailed description in equation 3), high strength and solidity, and low thermal dissipation. Major ultrasonic applications of high powers include cleaners, plastic welding, cutting, sewing, wire bonding, precious stone perforators, medical scalpels, and fish detectors or sonar.

However, the actuating frequency of an ultrasonic BLT vibrator is usually near resonance based on various equivalent models [1], but it is not constant. Being influenced by operating conditions on external loadings or working temperatures, the optimal frequencies have the shifting phenomena [2] resulting in resonant failure. To overcome the drawback, several servo driving circuits and controllers were developed with voltage feedback [3] or phase-lock-loop (PLL) technique [4]. Unfortunately, these complicated drive faced the difficult implementation for the purpose of commercial applications. Thus, we would like to introduce a novel driver of frequency adapting for an ultrasonic vibrator with motional current feedback, instead of the previous servo drive.

The optimal characteristic of electromechanical conversion is nearby resonance f_r for most kind of piezoelectric ceramics, where the maximum working current is obviously obtained. Therefore, the maximum output power is also generated at electromechanical resonance. In the past issues, the electric feature nearby resonant and anti-resonant frequencies was measured by a HP 4194A gain/phase impedance analyzer. The parameters of electrical components in the equivalent circuit were used to estimate dynamic electromechanical behaviors of a vibrator in frequency domain. Then, the equations of resonant frequency f_r and anti-resonant frequency f_a, based on a static equivalent circuit, could be expressed as [5]:

$$f_r = \frac{1}{2\pi\sqrt{L_m C_m}} \quad (1)$$

$$f_a = \frac{1}{2\pi\sqrt{L_m C_m C_0/(C_m + C_0)}} \quad (2)$$

where C_m and L_m represent the equivalent mechanical compliance ($1/k$) and the equivalent mass of a vibrator, respectively, and C_0 represents the damped capacitance. Also, k stands for the stiffness of a vibrator. The minimum and maximum magnitudes of impedance modulus of the BLT vibrator occur at the resonant fre-

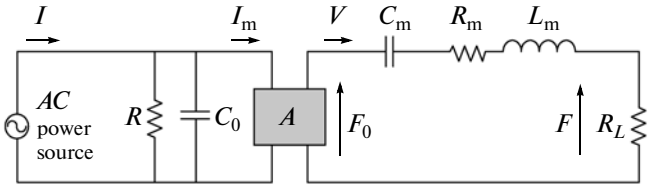

Fig. 1. Dynamic equivalent circuit of a vibrator [6].

quency and the anti-resonant frequency, respectively; i.e., in the point of energy view, maximum and minimum power output of the BLT vibrator is excited at the resonant frequency and the anti-resonant frequency, individually. Therefore, the function of quality factor Q_m is the ratio of electromechanical transformation and inversely proportional to internal energy loss R_m, calculated as

$$Q_m = \frac{\omega_r L_m}{R_m} = \frac{1}{\omega_r R_m C_m} \quad (3)$$

where ω_r is the angular frequency of a vibrator at resonance. Here, it is $\omega_r = 2\pi f_r$ (rad/sec). The resistance R_m represents the lump-sum loss of the mechanical damping and the dielectric loss. Furthermore, parameters of equivalent circuit, including R_m, L_m, C_m, C_0, f_r and f_a, are measured at a low voltage (1 V_{rms}) using a HP4194A impedance analyzer, and thus Q_m calculated by equation (3). Through the measurement of electrical feature, the vibrating amplitude and phase of BLT vibrators could be predicted based upon the parameter value of electrical components in an equivalent circuit. It was also applied to pre-determine the performance of BLT vibrators. Normally, resonant frequency f_r is major operating frequency for ultrasonic actuating systems. Equivalent circuits are usually simulated and experimented through electrical components for the design purpose of a driving circuit and control to an ultrasonic BLT vibrator.

Moreover, the dynamic equivalent circuit [6] could be constructed based on the motional current and micro vibration measurement through optical fiber [2], as shown in Fig. 1, where A represents the force factor, I_m denotes the motional current which is an excellent sensing target [7–9], and V is vibrating velocity of an vibrator. The electrical parameters of C_0 and R_0 represent dielectric loss and electrical energy loss in the electrical side, respectively. Also, R_m, L_m, and C_m are included in the mechanical side. Applying the measuring results of motional currents and micro-vibration, after also the calculation of the force factor A, the output power and efficiency in the mechanical side (right hand side) could be derived from the electrical side (left hand side) [10].

Thus, we expected that the mechanical output power is the multiplication of vibrating velocities and ended forces. Therefore, employing the measurement system to obtain the motional currents I_m and mechanical vibrating amplitude, the force factor A operating at high voltage or power could be computed as equation (4),

$$A = \frac{I_m}{\omega_r V_0} \quad (4)$$

where ω_r is the angular frequency of a vibrator at resonance, V_0 is the amplitude of mechanical vibration of an vibrator. After calculating the force factor, the equivalent parameters measured from an impedance analyzer can be converted into the practical operating parameters of the mechanical side via equation (5):

$$R_{mech} = R_m A^2 \quad (5a)$$

$$L_{mech} = L_m A^2 \quad (5b)$$

$$C_{mech} = \frac{C_m}{A^2} \quad (5c)$$

where R_{mech}, L_{mech}, and C_{mech} are counted into the bulk effect of force factor A as the real mechanical output for a vibrator.

When the input driving frequency is closer to the resonant frequency of a vibrator, the only R_m is left, due to the resonance, in the mechanical side of the equivalent circuit. Thus, through the calculation found in equation (6), the output force F of a vibrator could be [11]

$$F_0 = VA. \quad (6)$$

The direct and converse piezoelectric effect of an ultrasonic vibrator should be considered as energy conversion for a frequency drive with adapting function in this study, where an ultrasonic vibrator is the perturbation source to generate ultrasonic vibration. Based upon the detection of motional current where there is phase difference compared to driving voltages, the frequency adaptive drive is implemented and evaluated through experimental performance of external loading disturbances and working temperature interferences.

2. EXAMPLES OF ELECTROMECHANICAL COUPLING DESCRIBED BY MOTIONAL CURRENT

In practical applications, the ultrasonic vibrator is usually operated at 30 V_{pp} as a high power actuator. Therefore, there are different features exhibited in the HP analyzer measurement. For the characteristic evaluation and control purpose, the vibrating velocity and motional current are used as the feedback for a vibrator drive. By performing the integration of the vibrating velocity with time, the vibrating displacement could be obtained, which was compared to micro-vibration measurement through optical fiber detection.

Since the detection of motional currents is much easier than that of vibrating velocities, the motional current became the major measured parameter. Based on the equivalent circuit, the motional current I_m (that is, the current passing C_m–R_m–L_m components) is proportional to the vibrating velocity of a vibrator. Al-

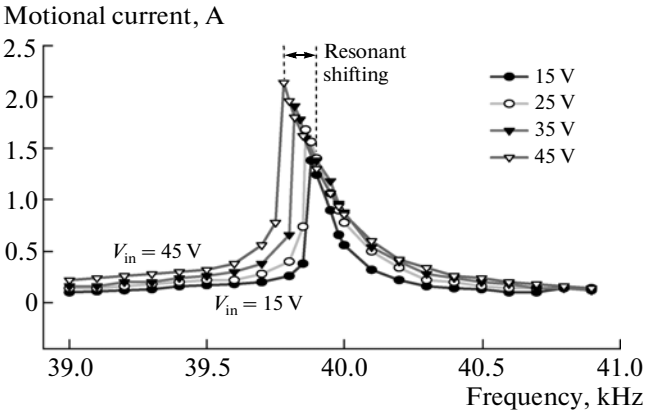

Fig. 2. Shifting phenomena of resonant frequencies based on motional current detection for a BLT vibrator.

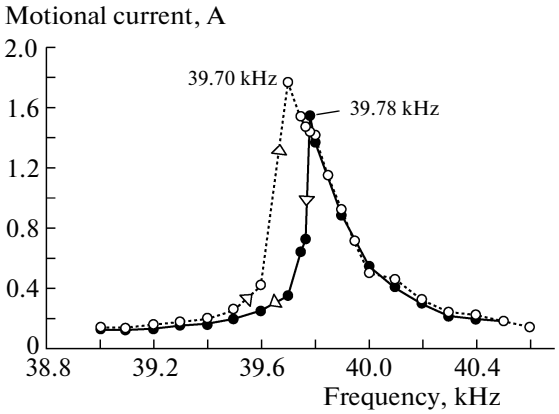

Fig. 3. Hysteresis loop of an ultrasonic vibrator.

so, the vibrating velocity was multiplied by end force to calculate the mechanical output powers of a vibrator. Thus, the vibrating velocities and displacements at the end of a vibrator can be predicted through the measurement of motional currents.

With high voltage input, the resonant frequency is shifted for a vibrator. The input voltage has a great effect on the resonant frequency as shown in Fig. 2. The resonant frequency is 39.9 kHz and 39.7 kHz driven at 15 V and 45 V respectively. There is difference of 200 Hz to drive the vibrator. The higher driving voltage has lower resonant frequency for a vibrator. The acceptable explanation is that the stiffness (k) of raw materials of a vibrator is no more the key term of the natural resonant frequency $\omega_n^2 (= m/k)$ while external voltage input. The piezoelectric effect was controlled by electrical field upon the mechanical stiffness to determine the excited resonant frequency, $\omega_{exc}^2 (= m/k_{PZT})$, where k_{PZT} stands for the electromechanical stiffness from the piezoelectric effect, instead of the natural resonant frequency ω_n. In other words, if much higher voltage is fed onto piezoelectric ceramics, the tough mechanical feature will come out from the piezoelectric effect resulting in the resonance frequency descent.

The piezoelectric ceramic has the special dynamic feature, known as the hysteresis phenomenon [12]. The resonant frequency of a vibrator has a different location based on driving frequencies going up or down as shown in Fig. 3. When the driving frequency is sent up, the resonant frequency is 39.70 kHz. Conversely, the resonant frequency is lifted up to 39.78 kHz during the back path of driving frequencies. There is 80 Hz difference during a driven vibrator. We believe that resonance with the least impedance contains great current through the piezoelectric materials and the current can generate the large thermal effect and mechanical vibration. These facts cause the shifting of resonant frequencies. Since the existence of mechanical deformation and output power are dominated by the converse piezoelectric effect, the largest deformation maybe reflect on thermal generation. The thermal generation causes not only the resonant frequency shifting, but also forms the existence of a hysteresis loop. The hysteresis loop could be easily detected via mechanical behaviors and motional currents.

3. CURRENT SENSOR FEATURE

Since the impedance of piezoelectric ceramics is minimized at resonance, the motional current can be an indicator as working status of an ultrasonic vibrator. Especially, the thermal effect or external loading variation becomes the system disturbance so that the resonant frequency has offset amount. In this study, a current transformer (CT) is used as a current sensor to detect the motional current as a feedback signal. Therefore, the phase difference between driving voltage and motional current could be monitored for adapting the optimal driving frequency nearby resonance. Through a core keeping all magnetic field and assembling as one set of coils, thus, the sensing magnetic force lines are transformed into the output voltage V_o as the feedback voltage (V_{pp}) and I_o as the shoot-through current (A_{pp}).

Usually, the linking coefficient K of an ideal CT type current sensor is expected as 100% for the transformation of voltage-current signals within ultrasonic bandwidth. However, due to magnet exciting current, magnetic leakage, ratio of magnetic permittivity and so on, the practical K value was measured as Fig. 4a shown. There is a linear zone from 100 Hz to 100 kHz within $K = 1.2$ range. After the sensing voltage is calibrated by the proper converting ratio, the output voltage V_o stands for the motional current of piezoelectric ultrasonic actuation. Hence, according the frequency feature of the CTL-6-P-Z type current sensor, it is very suitable as the feedback transducer for the drive of an ultrasonic vibrator. From Fig. 4b known, there is an excellent linear feature of output voltage V_o corre-

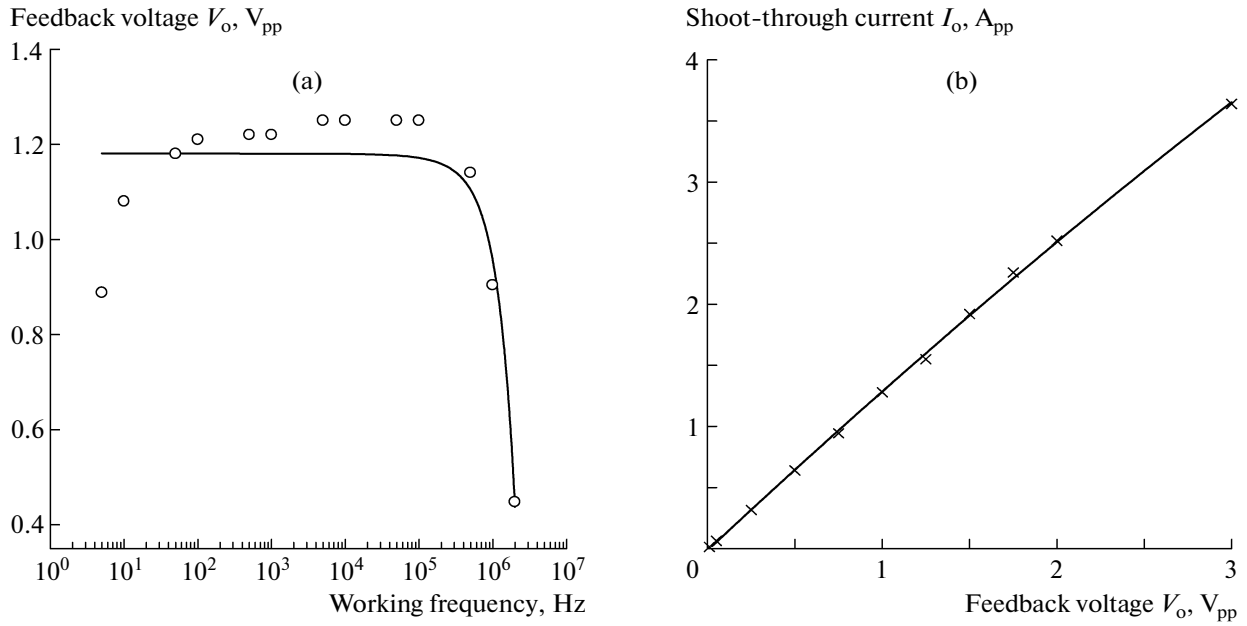

Fig. 4. Characteristics of current sensor: (a) Frequency characteristic of feedback voltage V_o of a CTL-6-P-Z type current sensor, and (b) Linear characteristic of feedback voltage V_o versus shoot-through current I_o.

sponding to shoot-through I_o for a CTL-6-P-Z current sensor. Therefore, both important features, including sensing error ratio (current sensing precision) and phase difference ratio (wave form accuracy), are always kept in a good quality during the motional current feedback.

4. DRIVER DESCRIPTION

The drive consists of a EM78M611 microcontroller integrated with a D/A converter (DAC10), a ICL8038 voltage controlled oscillator (VCO), a power amplifier, an A/D converter (ADC0820) and a current sensor, a voltage comparator (LM393) and signal coupling transformer as well as the signal attenuation and level tuning circuit [13–15], as shown in Fig. 5. This frequency adapting circuit applied a CT type sensor as feedback to detect the motional current for an ultrasonic vibrator.

After signal conditioning supporting signal attenuation and level shift circuit, the magnitude and phase degree of working voltages and motional currents were being processed by voltage comparators. Simultaneously, those instantaneous signals were fed into the microprocessor through analog-to-digital converter (ADC0820). The microprocessor determined the desired driving frequency and voltage based upon the feedback current magnitude as well as the phase difference compared to sensing voltage. The exactly calculated result was transferred into a digital-to-analog converter (DAC10) before the driving command sent into the voltage-controlled oscillator (VCO). Finally, the appropriate working frequencies and driving voltages were amplified by the power chip to actuate the ultrasonic vibrator.

4.1. Sensing circuit of signal attenuation and level shifting for current detection

Figure 6 illustrates the loading resistor R_L in series connection with a semi-variable resistor as an adjustable signal circuit for one of output terminals of the current sensor. Both resistors provide a tunable descending voltage for transforming current signals to proper voltage amplitude. Before voltage signals fed into the circuit of an attenuator and a level shifter, the operational amplifier OP_1 (LF357) plays a differential amplifier to get a correct DC voltage level $V_{cso1} = V_{ref} - V_{R_L}$ at 2.5 V which is inverting output signals from the current sensor.

4.2. Sensing circuit of signal attenuation and level shifting for voltage detection

Before voltage signals sensing from the current senor, a tuning circuit of signal attenuation and level shift was needed for fed a better signal to the voltage comparator within acceptable dynamic range, as shown in Fig. 7. Here, the output terminal of the power amplifier, V_{pa}, was connected to a coupling transformer T_1 where the circuit loop was constructed with the resistors R_1 and R_2. Hence, the divided voltage is representative for the attenuated signal before it is delivered to the operational amplifier OP_2 (LF357) with voltage output V_{po} as an impedance matched voltage follower. Also, the voltage level shifter consists of an

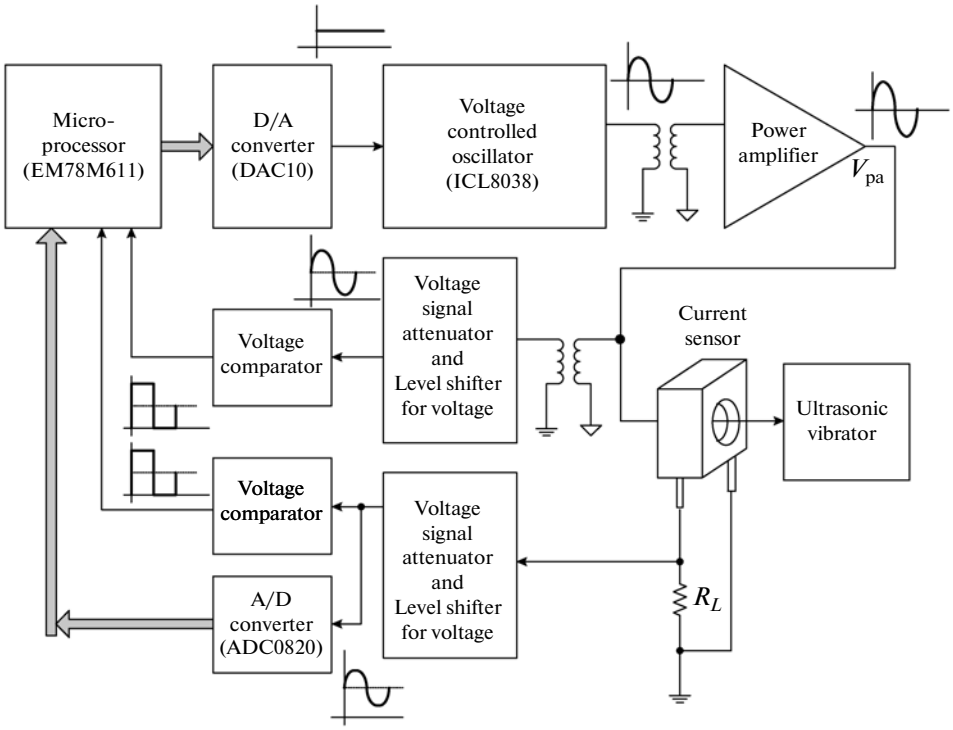

Fig. 5. Proposed driving circuit with motional current feedback for an ultrasonic vibrator.

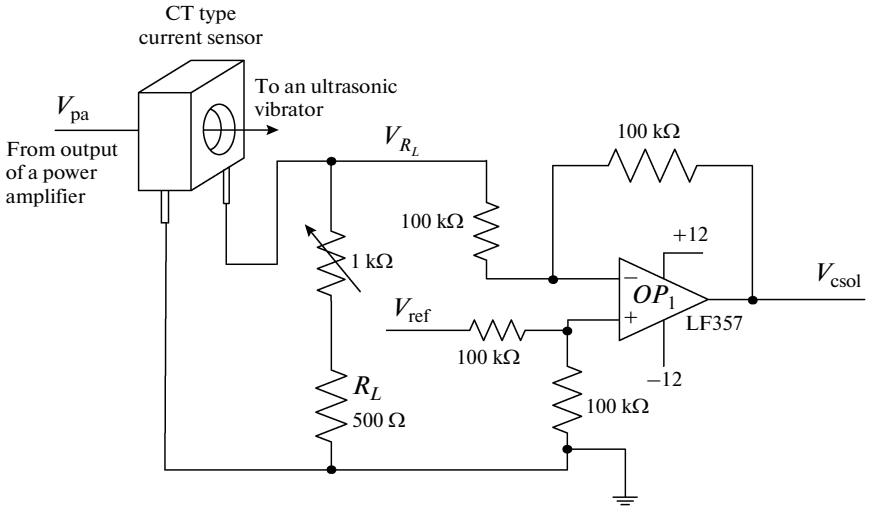

Fig. 6. Current sensing circuit consisted of a CT type sensor, signal attenuation and level shifting.

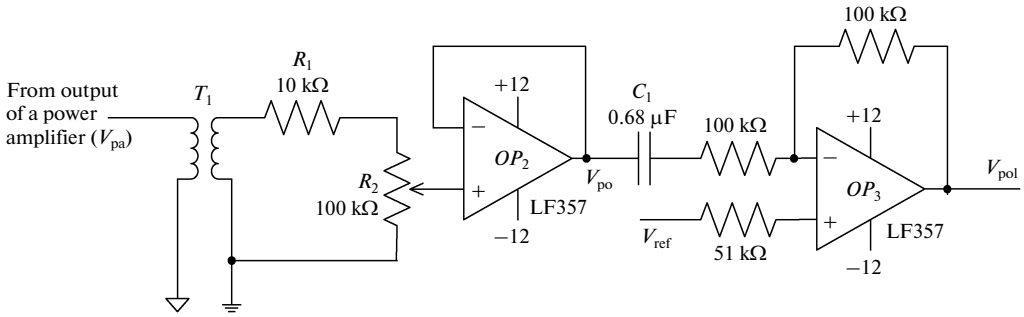

Fig. 7. Voltage sensing circuit of signal attenuation and level shifting.

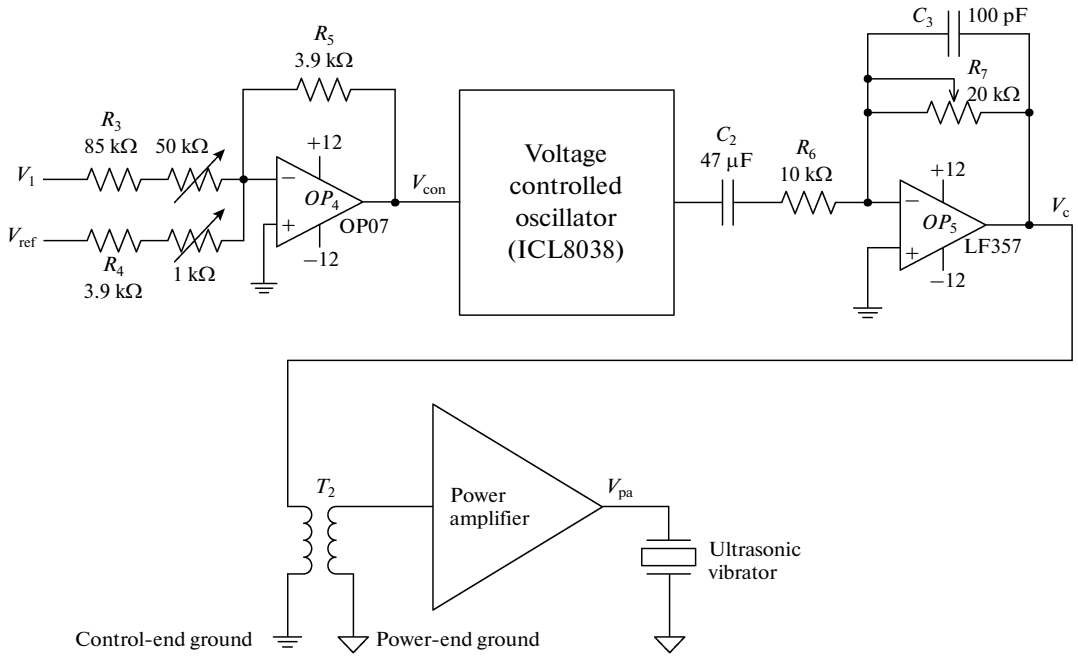

Fig. 8. Detailed tuning implementation of voltage-controlled-oscillator (VCO) circuit with an ICL8038 IC chip.

operational amplifier OP_3 (voltage output V_{po1}), resistors and a DC isolated capacitor.

4.3. Detailed tuning circuit of a voltage-controlled oscillator (VCO) for driving frequency

Figure 8 displays a voltage-controlled oscillating circuit which is broadly used to generate the desired waveform under various frequencies. The voltage-controlled chip (ICL8038) has the capability of wide band frequencies through external resistors and capacitors for sinusoidal, square, or triangle wave generation. In most case of 0.01–300 kHz range, the distortion ratio is less than 1% for sinusoidal wave output and the frequency-shifting onto temperature is about 250 ppm/°C. Employing a voltage V_1 from D/A converter (DAC10) as input signals, the inverted summing operational amplifier OP_4 (Texas Instruments, model OP07) performed the output as

$$V_{con} = -\left(\frac{R_5}{R_3}V_1 + \frac{R_5}{R_4}V_{ref}\right). \quad (7)$$

Because of the OP_4 output voltage from −2.42 to −2.58 V, the ICL8038 chip generates the sinusoidal wave from 37.8 to 39.8 kHz, i.e., each increment or decrement in one of the D/A converter output where the VCO would increase or reduce tuning less 2 kHz/step onto the working frequency. After tuning to the proper voltage level by the signal adjusting circuit OP_5 (National Semiconductor Inc., Model LF357), the driving voltage has the exact ultrasonic frequency fed into the signal-coupling transformer T_2 before driving the ultrasonic vibrator.

4.4. Brief algorithm in a microprocessor

The algorithmic concept for adapting frequency was implemented via the EM78M611 microprocessor based upon the signals of operating voltages and motional currents. The signals were detected by the current sensor to determine their phase difference through voltage comparators. According to the gain/phase of impedances, the phase degree is abruptly changed nearby either resonant frequency f_r or anti-resonant frequency f_a. There is a strong mechanism in energy conversion so that the sharp modification appeared in phase degree. For example, the phase degree suddenly reversed from 90° to 65° at resonant frequency f_r expresses that strong electrical capacitance of a piezoelectric vibrator is converted to electrical inductance of materials instantaneously in order to perform the task of electrical-mechanical conversion in energy. Thus, the microprocessor adjusted the voltage magnitude of various frequencies as input power source; i.e., the operating parameters were based on the instantaneous phase status of feedback currents compared to driving voltages for the working vibrator.

5. EXPERIMENTAL RESULTS AND DISCUSSION

After the initializing EM78M611 microprocessor at the specific driving frequency for the command of sinusoidal signal to modify VCO output through a D/A converter, the exactly desired frequency would be sent to the power amplifier for driving the vibrator. To acquire motional currents of a vibrator via a CT type sensor as feedback and to compare the phase offsets

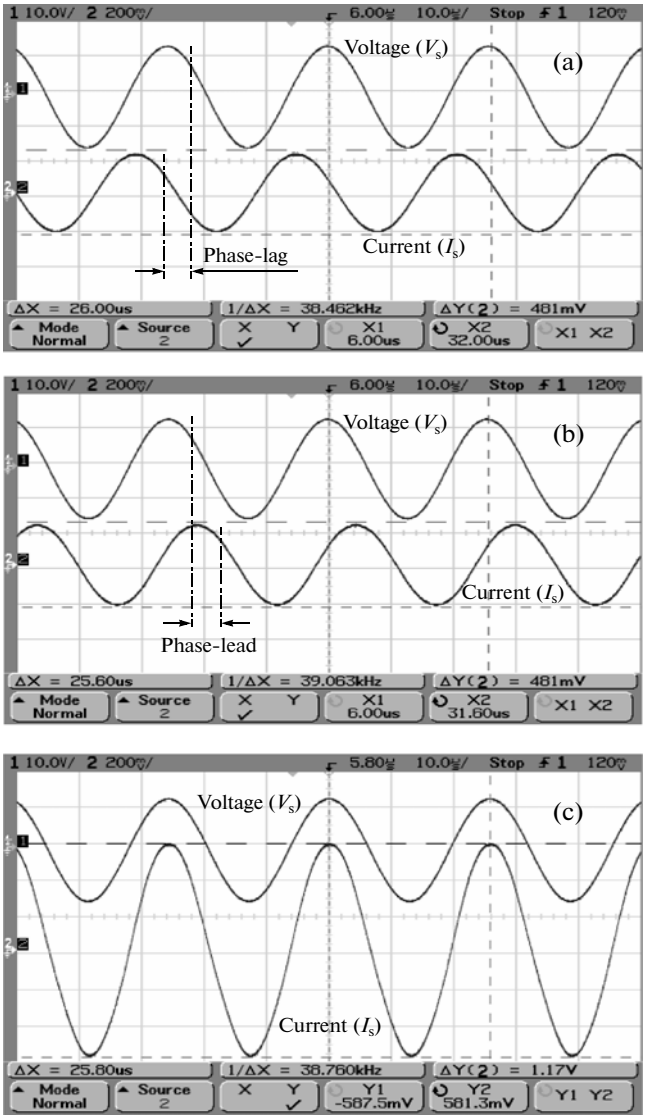

Fig. 9. Experimental wave forms of voltage and current detection: (a) Phase-lag case, (b) Phase-lead case, and (c) Corrected phase case by the frequency adapting strategy via the proposed drive.

among feedback currents and driving voltages through voltage comparators, the phase lead or phase lag could be evaluated by the micro-processor as shown in Fig. 9.

According the calculation of offsets for phase-lag either phase-lead cases, the optimal strategy would be produced to tune the output driving frequency of VCO for maintaining the maximum feedback currents. For example, Fig. 9a displays that the driving voltage V_s equals 30 V_{pp} as first channel (Ch1) acquiring and the feedback current I_s is at 481 mA_{pp} as second channel (Ch2) gaining. However, there is obvious phase lag; i.e., the calculating phase difference between V_s and I_s about –69.23° (~(–5 μs/26 μs) × 360°). It is capacitance feature of vibrator's equivalent circuit while driving voltages lagged feedback currents in phase degrees. Actually, the driving frequency (38.046 kHz) of the power source is little less than the resonant frequency (38.76 kHz) of the vibrator. Our tuning strategy would be voltage frequency arising from 2 Hz to 50 Hz added to the working frequency of the vibrator, depended on the feedback magnitude of motional currents. The D/A converter would receive the increment (1 to 25) from the EM78M611 microprocessor, resulting that the VCO chip sent higher driving frequencies (from 2 to 50 Hz) as the compensated amount added to working frequencies for vibrator operation [13].

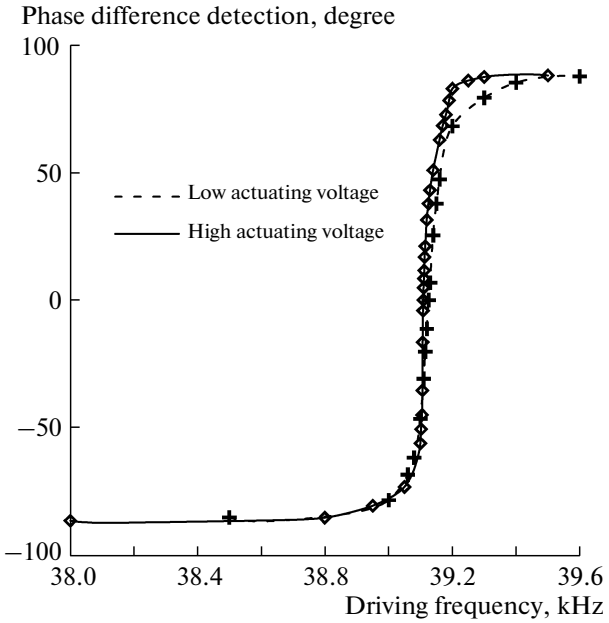

Fig. 10. Phase different based on the feedback of motional currents responding to sensing voltages nearby the actuating frequency via adapting strategies of the proposed drive.

For the phase-lead case as shown in Fig. 9b, the similar tuning strategy was adopted for compensated frequency shifting, except for reducing the amount of driving frequencies from 2 to 50 Hz, but depended on the critical magnitude of feedback currents. Figure 9c illustrates the well compensation in frequency shifting of the driven vibrator. Through the proper frequency tuning strategy based on the varied phase degrees, the micro-processor was monitoring continuously the working status of vibrators via the motional current feedback. Hence, the driving circuit supplies the appropriate driving frequency and electrical power for optimal vibrator driven.

The acceptable response relative to the resolution in the phase different detection of motional current feedback is kept by the novel adaptive drive as shown in Fig. 10. In either low or high actuating voltage, the adaptive drive is always dynamically tracing the optimal driving frequencies according to the actuating voltage modified from the variation of external disturbances, rather than the fixed driving frequency. Dur-

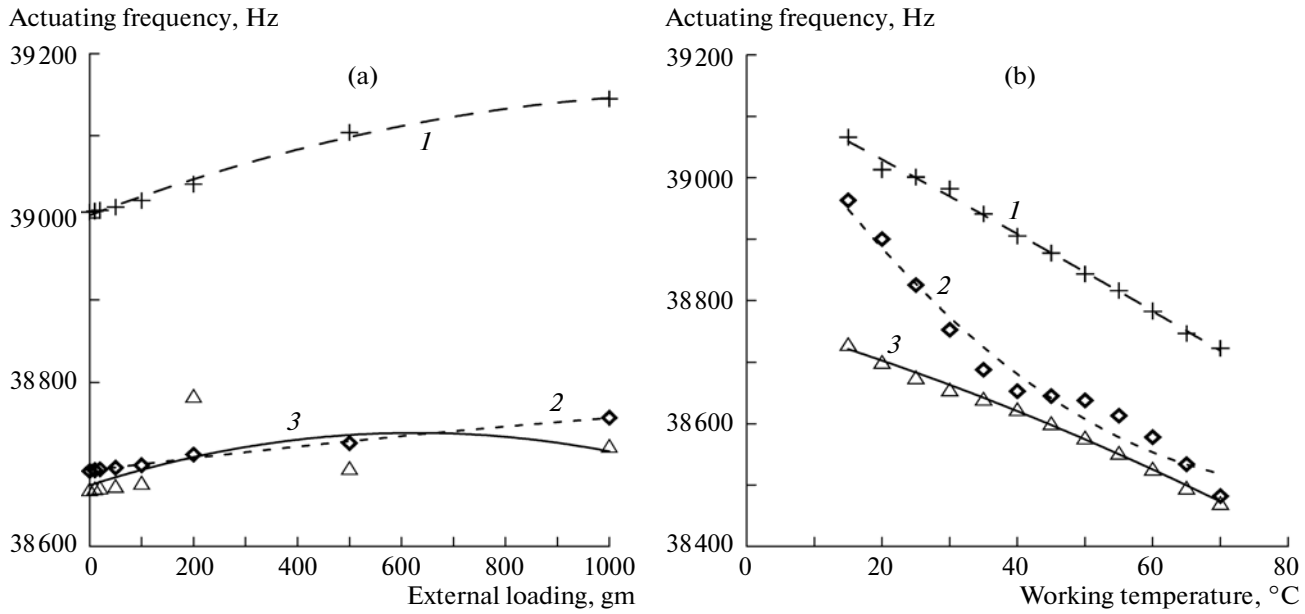

Fig. 11. Performance experiment for the drive with motional current feedback: (a) External loading disturbance, (b) Working temperature interference. *1* – driving voltage 10 V_{pp}, *2* – 30 V_{pp}, *3* – 50 V_{pp}.

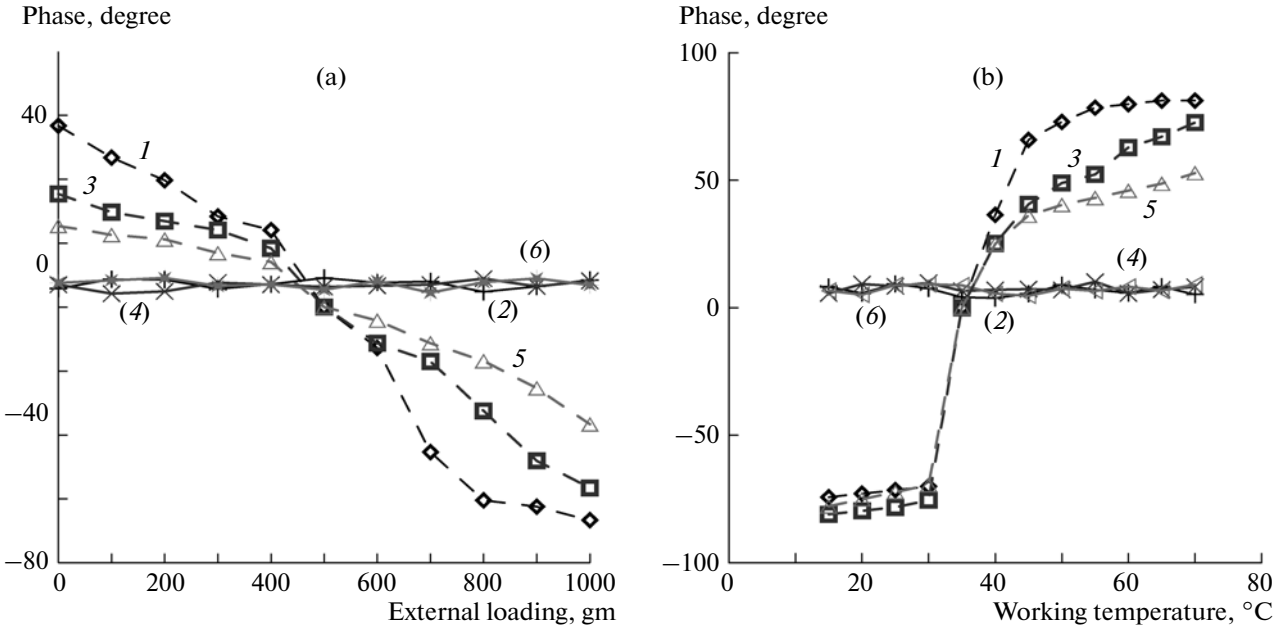

Fig. 12. Phase difference for the drive without/with motional current feedback: (a) External loading disturbance, and (b) Working temperature interference. *1*(*2*) – driving voltage 10 V_{pp} without feedback (with current feedback), *3*(*4*) – 30 V_{pp}, *5* (*6*) – 50 V_{pp}.

ing the zone of sharp slopes in phase difference, the adaptive drive has demonstrated the excellent resolution in proper feedback of motional currents.

Figure 11 illustrates performance experiment for the drive with frequency adapting circuit at various driving voltages onto an ultrasonic vibrator. There is a common tendency towards levitation in actuating frequencies while more external loading, except for the driving voltage 50 V_{pp} curve at 200 gm. The offset calculated in arithmetical average for the influence of external loading on frequencies is about 8.3 Hz per gram. The varied driving voltage interfered resonance in actuating frequency stronger than added external loadings as shown in Fig 11a. However, the drive demonstrates the excellent robust to reject these disturbances from external loadings, as shown in Fig. 12a. Due to

the motional current feedback, the phase difference in the driving resonant frequency is always keeping in the acceptable range (referred to solid lines), compared to without any feedback technique (referred to dash lines).

Since the frequency-thermal-shifting feature of a VCO ICL8038 chip was affected about 250 ppm/°C, the temperature coefficient corresponding to frequencies was about 9.75 Hz/°C for an ultrasonic vibrator working at 39 kHz as assumed original resonant frequency. Due to the contribution of adapting frequency strategy, high working temperature should not obviously affect the shifting of working frequencies, especially in driving voltage 50 V_{pp}, as shown in Fig. 11b. Although the thermal energy causes the electromechanical resonance in working frequencies going down, the experiment proves that the motional current feedback is an effective method for frequency tracking or adapting task to a high-power ultrasonic actuation, as shown in Fig. 12b. Therefore, the variation of driving frequencies, resulting from the thermal effect, would be compensated by the feedback of motional current using the frequency adapting circuit.

6. CONCLUSIONS

The instantaneous operating status is detected by a current sensor as feedback signals for the BLT vibrator drive. The optimal status in current sensing stands for an ultrasonic vibrator working in electromechanical coupling to perform the maximum mechanical output. After disturbance from external loading or temperature effect, the actuating frequency for the ultrasonic vibrator would be shifted, as well as the phase-lag or phase-lead case corresponding to frequencies could be also corrected through the motional current detection and tuning strategies. The driving circuit consists of a microprocessor, a voltage-controlled-oscillator (VCO) chip, an A/D-D/A converter and related signal conditioning circuits, where the motional current feedback has been implemented as the frequency adapting purpose. Each adapting signal, tuned by a VCO chip, is sent to a power amplifier to drive the ultrasonic vibrator in maximum output power.

Another advantage of the frequency adapting drive for an ultrasonic vibrator is easily improved by series connected with a resonant tank as a linear power amplifier. Thus, the improved frequency adapting drive could be applied to the industrial application in larger power consumptions, like ultrasonic clutches or ultrasonic assisted machining.

ACKNOWLEDGMENT

The work was supported in part by the National Science Council of Taiwan under grants # NSC-99-2918-I-129-001.

REFERENCES

1. Wen, F.L., and Hsu, I., *Instrum. Exp. Techn.,* 2011, vol. 54, no. 4, p. 488.
2. Umeda, M., Nakamura, and K., Ueha, S., *Jpn. J. Appl. Phys.*, 1999, vol. 38, p. 3327.
3. Lin, F.-J., Kuo, L.-C., *IEE Proc. Electr. Power Appl.*, 1997, vol. 144, no. 3, p. 199.
4. Lin, F.-J., Duan, R.-Y., and Yu, J.-C., *IEEE Trans. Power Electron.*, 1999, vol. 14, no. 1, p. 31.
5. Chang, K.-T., *Sensors and Actuators A*, 2007, vol. 133, p. 407.
6. Umeda, M., Nakamura, K., and Ueha S., *Jpn. J. Appl. Phys.*, 1998, vol. 37, p. 5322.
7. Lin, C.H., Chen, J. Y.H., and Wen, F.L., *IEICE Trans. Electronics*, 2005, vol. E88-C, no. 11, p. 2111.
8. Wen, F.L., Wen, C.-C., Chen, J. Y.H., and Ho, C.-Y., *Journal of the Chinese Institute of Engineers*, 2005, vol. 28, no. 6, pp. 949.
9. Wen, F.L., Wen, C.-C., Lai, M.-H., and Hsu, I., *IEICE Trans. on Electronics*, 2009, vol. E92-C, no. 8, pp. 1058.
10. Koike, Y., Tamura, T., and Ueha, S., *Jpn. J. Appl. Phys.*, 1997, vol. 36, p. 3121.
11. Hirose, S., *Jpn. J. Appl. Phys.*, 1994, vol. 33, p. 2945.
12. Petit, L., Rizet, N., Briot, R., and Gonnard, P., *Sensors and Actuators*, 2000, vol. 80, p. 45.
13. Data Sheet of DAC10 chips, Analog Devices, Inc., 1998.
14. Data Sheet of ADC0820 chips, National Semiconductor, Inc., 1999.
15. Data Sheet of ICL8038 chips, Intersil Corporation, 1999.